

## Molecular structures and antiproliferative activity of side-chain saturated and homologated analogs of 2-chloro-3-(*n*-alkylamino)-1,4-naphthoquinone



Sanjima Pal<sup>a</sup>, Mahesh Jadhav<sup>b</sup>, Thomas Weyhermüller<sup>c</sup>, Yogesh Patil<sup>d</sup>, M. Nethaji<sup>d</sup>, Umesh Kasabe<sup>b</sup>, Laxmi Kathawate<sup>b</sup>, V. Badireenath Konkimalla<sup>a,\*</sup>, Sunita Salunke-Gawali<sup>b,\*</sup>

<sup>a</sup> School of Biological Sciences, National Institute of Science Education and Research (NISER), Bhubaneswar 751 005, India

<sup>b</sup> Department of Chemistry, University of Pune, Pune 411 007, India

<sup>c</sup> MPI für Chemische Energiekonversion, Stiftstr. 34-36, 45470 Müllheim an der Ruhr, Germany

<sup>d</sup> Inorganic and Physical Chemistry Department, Indian Institute of Science, Bangalore, India

### HIGHLIGHTS

- Derivatives of 2-chloro-3-(*n*-alkylamino)-1,4-naphthoquinone are discussed.
- *n*-butyl, *n*-octyl derivative from polymeric chain through C—H...O and N—H...O close contacts.
- Molecules of *n*-hexyl derivative show dimer through N—H...O interaction.
- Antiproliferative activities were studied against in cancer cells of colon brain and pancreas.
- Tissue specific antiproliferative activity is observed for ethyl and for propyl derivative.

### ARTICLE INFO

#### Article history:

Received 1 June 2013

Received in revised form 24 June 2013

Accepted 24 June 2013

Available online 2 July 2013

#### Keywords:

$\pi$ - $\pi$  stacking

Aminonaphthoquinone

Hydrogen bonding

Antiproliferative activity

### ABSTRACT

Side chain homologated derivatives of 2-chloro-3-(*n*-alkylamino)-1,4-naphthoquinone (*n*-alkyl: pentyl; L-5, hexyl; L-6, heptyl; L-7 and octyl; L-8} have been synthesized and characterized by elemental analysis, FT-IR, <sup>1</sup>H NMR, UV-visible spectroscopy and LC-MS. Compounds, L-4, (*n*-alkyl: butyl; L-4), L-6 and L-8 have been characterized by single crystal X-ray diffraction studies. The single crystal X-ray structures reveal that L-4 and L-8 crystallizes in *P2*<sub>1</sub> space group, while L-6 in *P2*<sub>1</sub>/*c* space group. Molecules of L-4 and L-8 from polymeric chains through C—H...O and N—H...O close contacts. L-6 is a dimer formed by N—H...O interaction. Slipped  $\pi$ - $\pi$  stacking interactions are observed between quinonoid and benzenoid rings of L-4 and L-8. Orientations of alkyl group in L-4 and L-8 is on same side of the chain and polymeric chains run opposite to one another to form zip like structure to the alkyl groups. Antiproliferative activities of L-1 to L-8 (*n*-alkyl: methyl; L-1, ethyl; L-2, propyl; L-3 and butyl; L-4) were studied in cancer cells of colon (COLO205), brain (U87MG) and pancreas (MIAPaCa2) where L-1, L-2 and L-3 were active in MIAPaCa2 (L-1 = L-2 > L-3) and COLO205 (L-2 = L-3 > L-1) and inactive in U87MG. From antiproliferative studies with compounds L-1 to L-8 it can be concluded that homologation of 2-chloro-3-(*n*-alkylamino)-1,4-naphthoquinone with saturated methyl groups yielded tissue specific compounds such as L-2 (for MIAPaCa2) and L-3 (for COLO205) with optimal activity.

© 2013 Elsevier B.V. All rights reserved.

### 1. Introduction

Anthracyclines are a class of drugs used in cancer chemotherapy. They include doxorubicin, epirubicin and idarubicin. These compounds are used in treatment of many cancers, such as leukemias, lymphomas, breast, uterine, ovarian, and lung

cancers. All of these drug molecules contain quinone moieties in their framework. Quinonoid systems are related to their capacity to generate free radicals or semiquinones in redox reactions hence quinone derivatives have various pharmacological applications [1]. The clinical importance of 1,4-naphthoquinone has stimulated enormous interest in this class of compounds [2]. The synthesis of alkyl amino derivatives of 1,4-naphthoquinones is of prime interest, since these compound exhibit strong antibacterial [3], antimalarial and antitumor activity [4]. Furthermore, the amino-1,4-naphthoquinone moiety is the component of molecular framework of many natural products and has been used as synthetic key

\* Corresponding authors. Tel.: +91 2025601397x53; fax: +91 2025693981 (S. Salunke-Gawali), tel.: +91 9439864399; fax: +91 6742304121 (V.B. Konkimalla).

E-mail addresses: [badireenath@niser.ac.in](mailto:badireenath@niser.ac.in) (V.B. Konkimalla), [sunitas@chem.unipune.ac.in](mailto:sunitas@chem.unipune.ac.in) (S. Salunke-Gawali).

intermediate for synthesis of several compounds with important biological applications [5]. The amino and thioether substituted derivatives of 1,4-naphthoquinones possess extremely rich biological activities because of their redox potentials [5]. Single crystal X-ray structures of 1,4-naphthoquinone derivatives show molecular associations and the molecules forms three dimensional polymeric network through C—H...O and O—H...O hydrogen bonding and  $\pi$ - $\pi$  stacking interactions of benzenoid and quinonoid rings [6]. This molecular associations through hydrogen bonding may lead to stabilization of radical species and the redox cycling will decide the biological activity of 1,4-naphthoquinones.

Aminonaphthoquinone derivatives, 2-chloro-3-(*n*-alkylamino)-1,4-naphthoquinone (*n*-alkyl: pentyl; L-5, hexyl; L-6, heptyl; L-7 and octyl; L-8) (Scheme 1) are synthesized and characterized by various analytical tools in present investigation. Molecular associations of L-4, L-6 and L-8 are revealed by single crystal X-ray diffraction studies.

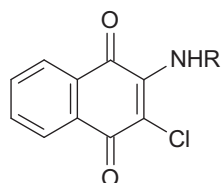
Till date several drugs are available in the market for chemotherapy but most of them have limited use due to unwanted and side/toxic effects. These side effects are mainly attributed to binding of the drug to unintended targets or tissues; urging a need for more tissue specific and potent therapeutics. Therefore, selectivity and specificity are the important parameters to be considered at a pre-screening level for identification potential anticancer lead compounds. Here in this study, antiproliferative activities of series of derivatives (*n*-alkyl: methyl; L-1, ethyl; L-2, propyl; L-3 and butyl; L-4) along with L-5 to L-8 derivatives were carried out against three cell lines COLO205 (human colorectal adenocarcinoma), U87MG (human primary glioblastoma) and MIAPaCa-2 (human pancreatic carcinoma) are studied. Further, the effect of homologation on the aminonaphthoquinone moiety (compounds L-1 to L-8) with respect to its tissue specific antiproliferative activity is reported in terms of degree of selectivity in the above-mentioned three cell lines.

## 2. Experimental

### 2.1. General materials and methods

The materials used viz. 2,3-dichloro-1,4-naphthoquinone, pentyl amine, hexyl amine, heptyl amine and octyl amine were purchased from Sigma–Aldrich. The reactant 2,3-dichloro-1,4-naphthoquinone have been recrystallized from methanol and used for further reactions. The solvents used such as dichloromethane, toluene, methanol were of analytical grade and purchased from Merck chemicals, India. Solvents were distilled in nitrogen atmosphere by standard methods [7] and dried where ever necessary.

FT-IR spectra of the compounds (Fig. S1) have been recorded between 4000–400  $\text{cm}^{-1}$  as KBr pellets on SHIMADZU FT 8400 spectrometer and  $^1\text{H}$  NMR of ligands (Fig. S2) are recorded in  $\text{CDCl}_3$  and  $\text{DMSO-}d_6$ , on Varian Mercury 300 MHz with TMS (tetramethylsilane) used as a reference. Elemental analysis has been performed on Thermo Finnigan EA 1112 Flash series elemental Analyzer. Mass of L-5 to L-8 has been determined using LC-MS 2010-eV (Make SHIMADZU). Melting points of L-5 to L-8 (Fig. S3) were determined



where,  
 L-1: R=CH<sub>3</sub>; L-2: R=C<sub>2</sub>H<sub>5</sub>; L-3:  
 R=C<sub>3</sub>H<sub>7</sub>; L-4: R=C<sub>4</sub>H<sub>9</sub>  
 L-5: R=C<sub>5</sub>H<sub>11</sub>; L-6: R=C<sub>6</sub>H<sub>13</sub>; L-  
 7: R=C<sub>7</sub>H<sub>15</sub>; L-8: R=C<sub>8</sub>H<sub>17</sub>

Scheme 1. Molecular formula of L-1 to L-8.

using melting point apparatus (Make- METTLER) and are corrected using DSC (Differential Scanning Calorimetry) technique (Make-METTLER, STAR SW 8.10).

### 2.2. X-ray crystallographic data collection and refinement of the structures

Single crystals of complexes L-4 and L-8 were coated with perfluoropolyether, picked up with nylon loops and were mounted in the nitrogen cold stream of the diffractometers. Monochromated Mo K $\alpha$  radiation (Bruker-AXS Kappa Mach3 with Incoatec Helios mirror,  $\lambda = 0.71073 \text{ \AA}$ ) from a Mo-target rotating-anode X-ray source was used for L-4. Intensity data of L-8 were collected on a Bruker AXS X8 Proteum diffractometer with focusing mirror optics (Cu K $\alpha$ ,  $\lambda = 1.54178 \text{ \AA}$ ). Final cell constants were obtained from least squares fits of several thousand strong reflections. Intensity data were corrected for absorption using intensities of redundant reflections with the program SADABS [8]. The structures were readily solved by direct methods and subsequent difference Fourier techniques. The Siemens ShelXTL [9] software package was used for solution and artwork of the structures, ShelXL97 [10] was used for the refinement. All non-hydrogen atoms were anisotropically refined and hydrogen atoms were placed at calculated positions and refined as riding atoms with isotropic displacement parameters. Crystallographic data of the compounds are listed in Table 1. Crystals of the L-6 suitable for diffraction studies were chosen carefully under a microscope. The unit cell parameters and the intensity data were collected on a Bruker SMART APEX CCD diffractometer, both equipped with a fine-focus Mo K $\alpha$  ( $\lambda = 0.71073 \text{ \AA}$ ) X-ray source. The SMART software was used for data acquisition and the SAINT software for data reduction. Absorption corrections were made using SADABS [8] program. The structure was solved and refined using the SHELXL-97 [10] programs. The crystal data was collected at room temperature and solved by direct methods. All the non-hydrogen atoms were refined anisotropically. Hydrogen atoms were located by difference Fourier synthesis and refined isotropically. Crystallographic data of the compounds are listed in Table 1.

### 2.3. Synthesis

All four L-5 to L-8, 2-chloro-3-(*n*-alkylamino)-1,4-naphthoquinones have been synthesized from 2,3-dichloro-1,4-naphthoquinone and using respective *n*-alkylamines. 1 g of 2,3-dichloro-1,4-naphthoquinone (4.4 mM) was dissolved in 25 ml of dichloro-

Table 1  
 Crystallographic data for complexes L-4, L-6 and L-8.

	L-4	L-6	L-8
Chem. formula	C <sub>14</sub> H <sub>14</sub> ClNO <sub>2</sub>	C <sub>16</sub> H <sub>18</sub> ClNO <sub>2</sub>	C <sub>18</sub> H <sub>22</sub> ClNO <sub>2</sub>
Fw	263.71	291.76	319.82
Space group	P2 <sub>1</sub> , No. 4	P2 <sub>1</sub> /c	P2 <sub>1</sub> , No. 4
a (Å)	7.3733(13)	5.512(1)	7.4007(5)
b (Å)	4.5915(8)	13.263(2)	4.7305(3)
c (Å)	18.024(3)	19.213(3)	22.8178(15)
$\beta$ (°)	90.853(3)	93.246(3) <sup>a</sup>	91.218(4)
V (Å <sup>3</sup> )	610.1(2)	1402.4(13)	798.65(9)
Z	2	4	2
T (K)	100(2)	293(2) K	100(2)
$\rho$ calcd (g cm <sup>-3</sup> )	1.435	1.382	1.330
refl. collected/ $2\theta_{\text{max}}$	17,161/61.42	12,010/27.7	16,798/127.38
unique refl./ $I > 2\sigma(I)$	3789/3551	3310	2544/2388
No. of params/restr.	168/1	253/0	204/1
$\lambda$ (Å/ $\mu(\text{K}\alpha)$ , cm <sup>-1</sup> )	0.71073/3.06	0.71073/2.73	1.54178/21.67
R1 <sup>a</sup> /goodness of fit <sup>b</sup>	0.0286/1.040	0.0490/1.073	0.0513/1.122
wR2 <sup>c</sup> ( $I > 2\sigma(I)$ )	0.0655	0.1135	0.1170
Residual density (eÅ <sup>-3</sup> )	+0.33/−0.20	+0.259/−0.265	+0.63/−0.42

methane and stirred for 15 min, which was then followed by drop wise addition of *n*-alkylamine solution (5.2 mM) L-5; pentyl amine, L-6; hexyl amine, L-7; heptyl amine, L-8; octyl amine). Reaction mixture has been stirred for 24 h. at room temperature (26 °C). Progress of reaction and purity of the ligands have been monitored by thin layer chromatography. Red color solids obtained by evaporation of the solvent. The crude product was purified by column chromatography in toluene: methanol (9:1) solvent system. The crystals for X-ray analysis are obtained by recrystallization in appropriate solvents.

### 2.3.1. Characterization of 2-chloro-3-pentylamino-1,4-naphthoquinone

L-5. Red crystals, 0.465 g (36.4%). m.p.: 97.1 °C. Anal. data calcd. for C<sub>15</sub>H<sub>16</sub>ClNO<sub>2</sub>: C, 64.87; H, 5.81; N, 5.04. Found C, 64.36; H, 5.78; N, 4.73. FT-IR (KBr,  $\nu_{\max}/\text{cm}^{-1}$ ): 3311, 2933, 2862, 1674, 1641, 1599, 1570, 1516, 1446, 1332, 1300, 1261, 1230, 1132, 1072, 1024, 895, 821, 723, 684, 650, 605, 563, 522, 447, 412. <sup>1</sup>H NMR; (300 MHz, DMSO-*d*<sub>6</sub>)  $\delta$ : 8.155 (d, 1H, *J* = 6 Hz), 8.033 (d, 1H, *J* = 7.8 Hz), 7.721 (t, 1H, *J* = 7.3 Hz), 7.620 (t, 1H, *J* = 7.9 Hz), 6.082 (br. s, 1H), 3.845(q, 2H, *J* = 6.8 Hz), 1.675 (m, 4H, *J* = 7.5 Hz), 1.388 (m, 4H, *J* = 6.3 Hz), 0.904 (d, 1H, *J* = 6.6 Hz). <sup>13</sup>C NMR; (500 MHz, DMSO-*d*<sub>6</sub>)  $\delta$ : 13.84, 21.79, 28.23, 30.45, 39.00, 43.85, 125.76, 126.45, 132.08, 132.55, 134.88, 145.11, 175.31, 180.15. UV-Vis; ( $\lambda_{\max}$ , nm, DMSO): 475, 338, 302. LC-MS (EI); *m/z*: 277.95 (M<sup>+</sup>+H).

### 2.3.2. Characterization of 2-chloro-3-hexylamino-1,4-naphthoquinone

L-6. Red crystals, 0.603 g (46.9%). m.p.: 84.95 °C. Anal. data calcd. for C<sub>16</sub>H<sub>18</sub>ClNO<sub>2</sub>: C, 65.86; H, 6.22; N, 4.8; Found C, 65.20; H, 6.23; N, 5.12. FT-IR (KBr,  $\nu_{\max}/\text{cm}^{-1}$ ): 3309, 3261, 2964, 2947, 2916, 2850, 1672, 1633, 1597, 1568, 1508, 1444, 1377, 1334, 1294, 1246, 1224, 1143, 1124, 1076, 1057, 999, 900, 821, 792, 725, 682, 644, 621, 547, 462, 432. <sup>1</sup>H NMR; (300 MHz, DMSO-*d*<sub>6</sub>)  $\delta$ : 8.155 (d, 1H, *J* = 7.2 Hz), 8.035 (d, 1H, *J* = 6.9 Hz), 7.720 (t, 1H, *J* = 7.2 Hz), 7.622 (t, 1H, *J* = 7.0 Hz), 6.078 (br. s, 1H), 3.845(q, 2H, *J* = 6.8 Hz), 1.664 (m, 5H, *J* = 7.5 Hz), 1.331 (m, 5H, *J* = 8.5 Hz), 0.880 (d, 1H, *J* = 6.9 Hz). <sup>13</sup>C NMR; (500 MHz, DMSO-*d*<sub>6</sub>)  $\delta$ : 13.82, 21.98, 25.70, 30.73, 30.89, 39.17, 39.93, 40.01, 43.90, 125.78, 126.48, 132.09, 132.575, 134.90, 180.18 UV-Vis; ( $\lambda_{\max}$ , nm, DMSO): 476, 338, 301. LC-MS (EI); *m/z*: 291.95 (M<sup>+</sup>+H).

### 2.3.3. Characterization of 2-chloro-3-heptylamino-1,4-naphthoquinone

L-7. Red crystals, 0.577 g (42.8%). m.p.: 86.69 °C. Anal. data calcd. for C<sub>17</sub>H<sub>20</sub>ClNO<sub>2</sub>: C, 66.77; H, 6.59; N, 4.58; Found C, 68.81; H, 6.67; N, 4.73; FT-IR (KBr,  $\nu_{\max}/\text{cm}^{-1}$ ): 3313, 2926, 2856, 1674, 1641, 1599, 1568, 1514, 1442, 1371, 1330, 1298, 1259, 1163, 1132, 1072, 1022, 871, 821, 721, 682, 650, 603, 563, 526, 441. <sup>1</sup>H NMR; (300 MHz, DMSO-*d*<sub>6</sub>)  $\delta$ : 8.154 (d, 1H, *J* = 7.5 Hz), 8.036 (d, 1H, *J* = 7.8 Hz), 7.728 (t, 1H, *J* = 7.5 Hz), 7.621 (t, 1H, *J* = 7.6 Hz), 6.085 (br. s, 1H), 3.844(q, 2H, *J* = 7.0 Hz), 1.688 (m, 4H, *J* = 7.1 Hz), 1.578 (d, 4H, *J* = 8.2 Hz), 1.333 (m, 4H, *J* = 8.2 Hz), 0.884 (d, 1H, *J* = 6.7 Hz). <sup>13</sup>C NMR; (500 MHz, DMSO-*d*<sub>6</sub>)  $\delta$ : 13.88, 21.98, 25.98, 28.32, 30.74, 31.14, 43.88, 125.78, 126.47, 129.83, 132.09, 132.57, 134.90, 145.14, 145.34, 175.33, 180.18. UV-Vis; ( $\lambda_{\max}$ , nm, DMSO): 476, 338, 300. LC-MS (EI); *m/z*: 305.95 (M<sup>+</sup>+H).

### 2.3.4. Characterization of 2-chloro-3-octylamino-1,4-naphthoquinone

L-8. Red crystals, 0.591 g (41.7%). m.p.: 89.95 °C. Anal. data calcd. for C<sub>18</sub>H<sub>22</sub>ClNO<sub>2</sub>: C, 67.60; H, 6.93; N, 4.38; Found C, 67.05; H, 6.88; N, 4.39; FT-IR (KBr,  $\nu_{\max}/\text{cm}^{-1}$ ): 3313, 2924, 2854, 1674, 1641, 1597, 1570, 1514, 1442, 1371, 1330, 1298, 1259, 1132, 1072, 1003, 823, 721, 684, 650, 565, 530. <sup>1</sup>H NMR; (300 MHz, DMSO-*d*<sub>6</sub>)  $\delta$ : 8.157 (d, 1H, *J* = 7.8 Hz), 8.034 (d, 1H, *J* = 7.5 Hz), 7.727 (t, 1H, *J* = 7.3 Hz), 7.622 (t, 1H, *J* = 7.6 Hz), 6.083 (br. s, 1H), 3.848(q, 2H, *J* = 6.8 Hz), 1.697 (m, 2H, *J* = 7.1 Hz), 1.475 (m, 2H,

*J* = 7.9 Hz), 1.378 (m, 2H, *J* = 3.4 Hz), 0.931 (d, 1H, *J* = 7.2 Hz). <sup>13</sup>C NMR; (500 MHz, DMSO-*d*<sub>6</sub>)  $\delta$ : 13.87, 22.02, 25.98, 28.53, 28.59, 30.70, 31.14, 39.34, 39.51, 40.05, 43.95, 125.77, 126.46, 128.91, 132.08, 132.56, 134.89, 180.17. UV-; ( $\lambda_{\max}$ , nm, DMSO): 476, 338, 300. LC-MS (EI); *m/z*: 319.95 (M<sup>+</sup>+H).

## 2.4. Cell lines

COLO205 (human colorectal adenocarcinoma), U87MG (human primary glioblastoma) and MIAPaCa2 (human pancreatic carcinoma) cell lines were obtained from National Centre for Cell Science (Pune, India). COLO205 cell line was cultured routinely in RPMI-1640 medium (HiMedia, India) while U87MG and MIAPaCa2 in DMEM media. Both media were supplemented with 2 mM glutamine (Himedia, India), antibiotics (100  $\mu$ /mL penicillin A and 100  $\mu$ /mL streptomycin; Himedia, India) and 10% heat-inactivated fetal bovine serum (HiMedia, India). All cell lines were cultured in 25 cm<sup>2</sup> flasks with loosened caps and incubated in humidified air containing 5% CO<sub>2</sub> at 37 °C. Origin pro software and MS-Excel were used for data analysis.

## 2.5. XTT assay for anti-proliferative activity

The effect of isolated L-1 to L-8 on the viability of the cell lines were measured using XTT assay. The cytotoxicity were evaluated based on the amount of 2,3-bis[2-methoxy-4-nitro-5-sulfophenyl]-2H-tetrazolium-5-carboxanilide inner salt formed by the viable cells in the treated wells. Fresh stock solutions of 3 and 4 were prepared in DMSO at a concentration of 100 mM. Serial dilution in 50:50; media: DMSO mixtures produced stock solutions of compounds ranging from 10<sup>-8</sup> M to 10<sup>-4</sup> M. About 50  $\mu$ L of the cell suspension diluted to a final density of 1  $\times$  10<sup>5</sup> cells/mL were sowed into each well of a 96-well culture plate (Axygen, USA) and treated with the varying concentrations of compounds in duplicates. The compound treated 96-well plates were left for incubation at 37 °C and 5% CO<sub>2</sub> in humidified atmosphere for 72 h. XTT reagent mixture was freshly prepared with XTT-labeling reagent and electron-coupling reagent in a ratio of 50:1. Post 72 h of incubation, 50  $\mu$ L of this mixture was added to each of the 96 wells. The plates were incubated at 37 °C, 5% CO<sub>2</sub> in humidified atmosphere and read out after optimal color development in each of the wells. Quantification of cell viability was performed in an ELISA plate reader (Bio-Rad, München, Germany) at 490 nm with a reference wavelength of 655 nm. The above-mentioned cell lines treated with doxorubicin served as a positive control for cytotoxicity and to evaluate the same [11,12].

## 3. Result and discussion

Biological activity of quinones depends on their ortho- and para- tautomeric form [13]. Three mechanisms were proposed to cytotoxic activity of quinones in various biological systems [14]. These mechanisms involve generation of active oxygen species by redox cycling, intercalation between nucleotides in the DNA double helix or alkylation of biomolecules. Quinones generally accepts one and two electrons by redox cycling to form *in situ* corresponding radical anion and dianions species respectively, this creates intracellular hypoxic conditions due to excess of superoxide radical [14a]. This radical will be converted to hydrogen peroxide by superoxide dismutase enzyme or it may form hydroxyl radical by Fenton reaction[14b,c]. These oxygen intermediates or reactive oxygen species (ROS) may react directly with DNA or other biomolecules such as proteins and lipids, which leads to cell damage [14g,h]. Cytotoxicity of quinones to mammalian and cancer cells can also be explained due inhibition of topoisomerases, a

group of enzyme that are important for DNA replication in cells [14f].

Biological activity of the quinones could also be related to their interactions with biomolecules. Noncovalent interactions and  $\pi$ - $\pi$  stacking ability of quinone derivatives will play major role in binding of quinone molecules to the biomolecules [15]. Single crystal structures of several previously reported [6] naphthoquinone ligands are polymeric in nature where intermolecular C—H...O, O—H...O and N—H...O interactions were common in these ligands. Some of them do possess  $\pi$ - $\pi$  stacking interactions, which could help them to intercalate with DNA.

To reveal their roles in molecular interactions besides redox cycling, we have synthesized homologated series of aminonaphthoquinone viz. 2-chloro-3-(*n*-alkylamino)-1,4-naphthoquinone. Although redox cycling is present in all compounds of homologated series, however their molecular interactions viz. hydrogen bonding and  $\pi$ - $\pi$  stacking interactions may vary and this will affect their tissue specific antiproliferative activity.

### 3.1. Synthesis and characterization of homologated, 2-chloro-3-(*n*-alkylamino)-1,4-naphthoquinone

Ligands L-5 to L-8 are purified by column chromatography using toluene and methanol as solvents and purity have been determined by LC-MS experiments and purity of all the compounds is >99.5%. Melting points of L-5 to L-8 were corrected by Differential Scanning Calorimetry (DSC) (Fig. S3).

$\nu_{\text{N-H}}$  vibrations are observed in FT-IR spectra  $\sim 3300 \text{ cm}^{-1}$  and  $\nu_{\text{C=O}}$  vibration frequency is observed  $\sim 1674 \text{ cm}^{-1}$  [6b]. The characteristics of paranaphthoquinone (p-NQ) vibrations are observed  $\sim 1260 \text{ cm}^{-1}$  in L-5, L-7 and L-8, while these vibrations are decreased by  $\sim 15 \text{ cm}^{-1}$  in L-6. p-NQ vibrations are susceptible to strength of intermolecular hydrogen bonding. UV-vis spectra of L-5 to L-8 (Fig. S4) in DMSO show two bands in UV region viz.  $\sim 301 \text{ nm}$  and  $338 \text{ nm}$  are assigned to  $\pi$ - $\pi^*$  transitions of naphthoquinone ring and a broad band between 400 and 600 nm is

assigned to  $n$ - $\pi^*$  charge transfer transition [16], this imparts red color to all the compounds.

### 3.2. X-ray crystal structures of L-4, L-6 and L-8

L-1 and L-3 crystallizes in triclinic space group *P*-1, while L-2 crystallizes in orthorhombic space group *Pca*2 (CCDC 907096-907098). L-1 to L-3 shows, intra (N—H...O) as well as intermolecular (N—H...O and C—H...O) hydrogen bonding interactions. Quinonoid rings of adjacent chains in L-1 and L-3 are  $\pi$ - $\pi$  stacked, while this interaction is absent in L-2.

ORTEP plots of L-4, L-6 and L-8 are shown in Fig. 1a–c respectively and crystallographic data is represented in Table 1. L-4 and L-8 crystallizes in monoclinic space group *P*2<sub>1</sub>/c, No. 4, while L-6 crystallizes in *P*2<sub>1</sub>/c (Table 1). Carbonyl bond distances are within range of oxidized form of naphthoquinone ligands [17] (Tables S1–S3). C—N distance is  $\sim 1.34 \text{ \AA}$  is also within range while L-6 crystallizes in *P*2<sub>1</sub>/c (Table 1). Carbonyl bond distances observed for similar to aminonaphthoquinone ligands while C(2)—C(3) bond distance is observed to be longer as compared to similar aminonaphthoquinone ligands [18].

Inter molecular hydrogen bonding interaction is observed in L-4, L-6 and L-8 (Table 2). Molecular structures of L-4 and L-8 are hydrogen bonded polymer while molecular structure of L-6 is a dimer. Although L-4 and L-8 crystallizes in the same space group, their hydrogen bonding interactions are differs.

Bifurcated intermolecular hydrogen bonding is observed to O(1) in L-4. Molecules of L-4 form polymeric chain through C—H...O and N—H...O interactions [19] (Fig. 2a). Orientations of alkyl group when viewed down *b*-axis, is on same side of the chain while the polymeric chains runs opposite to one another and zip like structure is formed to the alkyl groups of the neighboring chains. Slipped  $\pi$ - $\pi$  stacking interaction (Fig. S5) are observed between benzenoid and quinonoid rings; C(1),C(9) [3.362 Å] and C(1), C(8) [3.359 Å].

Molecules of L-8 form polymeric chain through C—H...O and N—H...O interaction (Fig. 2c). An orientation of alkyl groups are

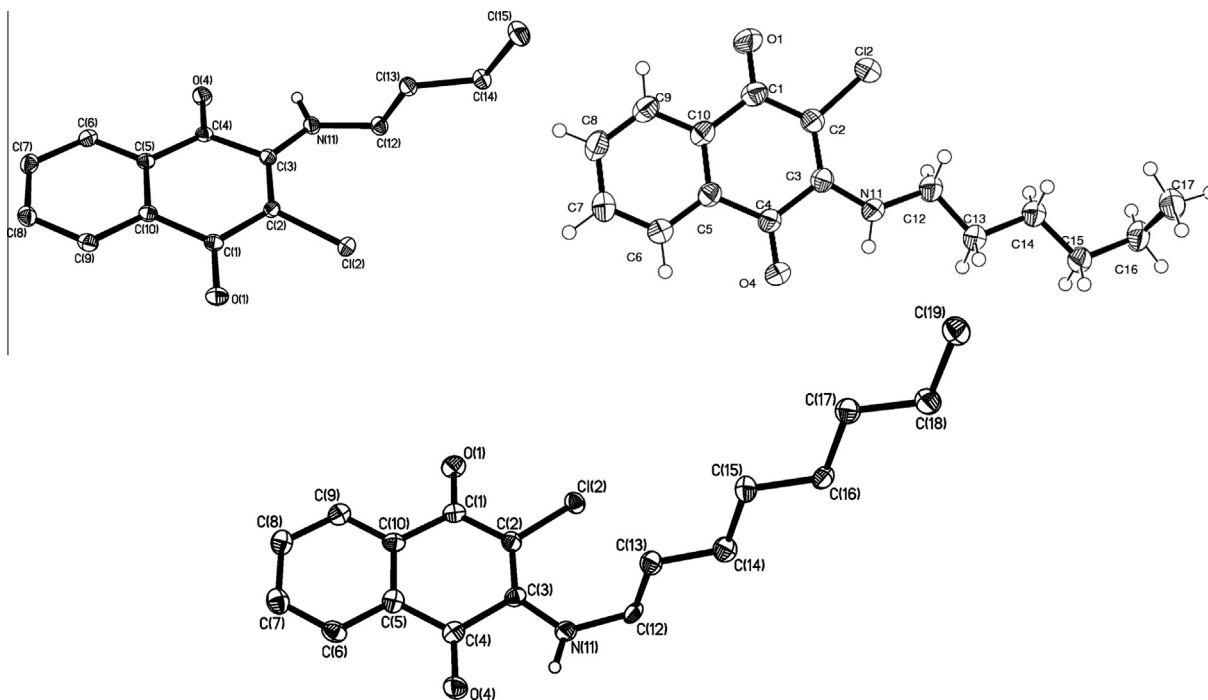
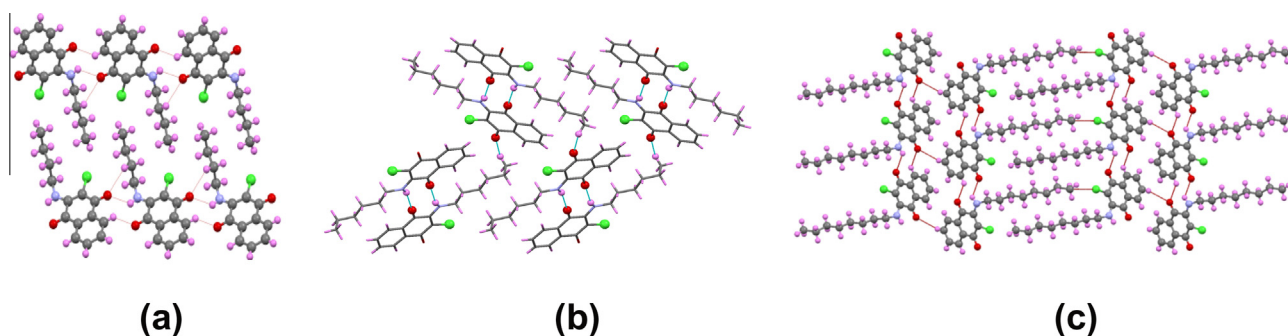


Fig. 1. ORTEP plots of: (a) L-4, (b) L-6 and (c) L-8.

**Table 2**  
Hydrogen bond geometries for L-4, L-6 and L-8.

	Sr. no	D—H...A	D—H(Å)	H...A(Å)	D...A(Å)	D—H...A(°)
L-4	1	N(11)—H(11)...O(1) <sup>i</sup>	0.820(2)	2.320(2)	2.935(2)	132(2)
	2	C(9)—H(9)...O(4) <sup>ii</sup>	0.951(1)	2.548(1)	3.242(2)	130(1)
	3	C(13)—H(13)B...O(1) <sup>iii</sup>	0.950(1)	2.609(1)	3.337(2)	130(1)
L-6	4	N(11)—H(11)...O(4) <sup>iv</sup>	0.840(2)	2.650(2)	3.458(2)	163(2)
	5	C(17)—H(17A)...O(1) <sup>v</sup>	0.990(3)	2.600(2)	3.384(3)	136(2)
L-8	6	N(11)—H(11)...O(1) <sup>ii</sup>	0.880(4)	2.310(2)	2.945(4)	129(4)
	7	C(9)—H(9)...O(4) <sup>ii</sup>	0.950(4)	2.562(1)	3.257(5)	130(2)
		C(7)—H(7)...O(4) <sup>vi</sup>	0.949(5)	2.708(1)	3.297(4)	121(1)

(i)  $-1+x,y,z$ ; (ii)  $1+x,y,z$ ; (iii)  $-x,1/2+y,-z$ ; (iv)  $-x,-y,-z$ ; (v)  $1+x,1/2-y,1/2+z$ ; (vi)  $2-x,-1/2+y,1-z$ .

**Fig. 2.** Molecular packing in: (a) L-4, down *b*-axis; (b) L-6 down *a*-axis and (c) L-8 down *b*-axis.

on same side of the chain and the two polymeric chain runs opposite to one another. The chains are further intermolecular hydrogen bonded through C—H...O interactions [C(7)—H(7)...O(4)]. There is slipped  $\pi$ - $\pi$  stacking interaction is observed between C1 and C(1), C(10) and C(1), C(8) [ $x, 1+y, z$ ] (Fig. S6).

Molecules of L-6 form dimers through N—H...O(1) interaction (Fig. 2b). Orientations of molecules are 'anti' to one another. The dimers further interlinked by C—H...O interaction.

Molecular structures of homologated series vary with respect to  $\pi$ - $\pi$  stacking and hydrogen bonding interactions. This variation in molecular interactions could affect the biological properties in

homologated series. Quinonoid as well as benzenoid rings are involved in  $\pi$ - $\pi$  stacking interactions. Molecules of L-1 and L-3 show  $\pi$ - $\pi$  stacking of the quinonoid rings of the neighboring chains while, molecules of L-4 and L-8 shows slipped  $\pi$ - $\pi$  stacking interaction between benzenoid and quinonoid rings in a chain and molecules of L-2 and L-6 do not possess  $\pi$ - $\pi$  stacking interactions.

### 3.3. Antiproliferative activities

Table 3 illustrates the IC<sub>50</sub> values obtained from cell proliferation studies on three carcinoma cell lines (COLO205, U87MG and MIA-PaCa2). Compounds L-1 to L-8 has no effect on the brain tumor type (U87MG) but in case of COLO205 and MIA-PaCa2, compounds with carbon chain  $\geq 3$  (C = 4, 5, 6, 7 and 8; L-4 to L-8) were inactive in all three cell lines.

In COLO205, an increase in activity was observed from L-1, L-2 and L-3 (C = 1, 2 and 3 respectively) and no effect from L-4 to L-8 indicating L-3 to be an optimal structure for antiproliferative activity in COLO205 cell line (Table 4). Whereas, a *vice versa* was observed in MIA-PaCa2 for L-1 to L-3 where a decrease in the antiproliferative activity and no effect from L-4 to L-8 indicating L-2 as an optimal structure of antiproliferative activity in MIA-PaCa2 (Table 4). Treatment of cell lines with doxorubicin showed marked increase in antiproliferative activity non-specifically in all three cases.

**Table 3**  
Effect of homologation on antiproliferative for L-1 to L-8 in COLO205, U87MG and MIA-PaCa2 in terms of IC<sub>50</sub>.

Compound	Carbon chain	COLO205	U87MG	MIA-PaCa2
L-1	—CH <sub>3</sub>	223 ± 3.5 $\mu$ M	>100 mM	11.5 ± 6.2 $\mu$ M
L-2	—C <sub>2</sub> H <sub>5</sub>	91.4 ± 9.5 $\mu$ M	>100 mM	12.8 ± 8 $\mu$ M
L-3	—C <sub>3</sub> H <sub>7</sub>	92.2 ± 12 $\mu$ M	>100 mM	1.3 ± 2 mM
L-4	—C <sub>4</sub> H <sub>9</sub>	>100 mM	>100 mM	>100 mM
L-5	—C <sub>5</sub> H <sub>11</sub>	>100 mM	>100 mM	>100 mM
L-6	—C <sub>6</sub> H <sub>13</sub>	>100 mM	>100 mM	>100 mM
L-7	—C <sub>7</sub> H <sub>15</sub>	>100 mM	>100 mM	>100 mM
L-8	—C <sub>8</sub> H <sub>15</sub>	>100 mM	>100 mM	>100 mM
Doxorubicin		67.8 ± 0.25 nM	0.34 ± $\mu$ M	0.07 ± 0.4 nM

**Table 4**  
Correlation of homologation of L-1, L-2 and L-3 compounds to degree of specificity to COLO205 and MIA-PaCa2 cell line.

	Carbon chain	Degree of specificity <sub>COLO205</sub> <sup>*</sup>	Degree of specificity <sub>MIA-PaCa2</sub> <sup>#</sup>
L-1	—CH <sub>3</sub>	0.05	19.39
L-2	—C <sub>2</sub> H <sub>5</sub>	0.14	7.14
L-3	—C <sub>3</sub> H <sub>7</sub>	14.10	0.07

<sup>\*</sup> Degree of specificity<sub>COLO205</sub> = IC<sub>50</sub>(MIA-PaCa2)/IC<sub>50</sub>(COLO205).

<sup>#</sup> Degree of specificity<sub>MIA-PaCa2</sub> = IC<sub>50</sub>(COLO205)/IC<sub>50</sub>(MIA-PaCa2).

### 3.4. Correlation of homologation to degree of specificity

The degree of specificity for a cancer tissue type was determined from the IC<sub>50</sub> values obtained from antiproliferative studies activity studies and correlated with the homologation on the active derivatives of aminonaphthoquinones (L-1, L-2 and L-3) from Table 4, it can be concluded that homologation of 2-chloro-3-(*n*-alkylamino)-1,4-naphthoquinone with saturated propyl group (L-3, C = 3) has 14 times more activity against colon cancer than pancreas. Whereas a shift in the tissue selectivity of about 19 times more activity was observed in pancreas when substituted with methyl group (L-1, C = 1).

## 4. Conclusion

Side chain homologated derivatives of 2-chloro-3-(*n*-alkylamino)-1,4-naphthoquinone (*n*-alkyl: pentyl; L-5, hexyl; L-6, heptyl; L-7 and octyl; L-8) have been synthesized and characterized in this investigation. Molecular structures of L-4, L-6 and L-8 have been evaluated by single crystal X-ray diffraction studies. Intra as well as intermolecular hydrogen bonding interaction is observed in L-4, L-6 and L-8. Molecules of L-6 form dimers through N—H···O interactions while, L-4 and L-8 show slipped  $\pi$ – $\pi$  stack interaction between quinonoid and benzenoid rings.

Antiproliferative activities of L-1 to L-8 (*n*-alkyl: methyl; L-1, ethyl; L-2, propyl; L-3 and butyl; L-4) were studied in cancer cells of colon (COLO205), brain (U87MG) and pancreas (MIAPaCa2). From antiproliferative studies on the colon, pancreas and brain cell lines with compounds L-1 to L-8 it can be concluded that homologation of 2-chloro-3-(*n*-alkylamino)-1,4-naphthoquinone with saturated methyl groups yielded tissue specific compounds such as L-1 (for MIAPaCa2) and L-3 (for COLO205) with optimal activity. With increase in alkyl groups of side chain homologated series, will decrease the redox potential of naphthoquinone/naphthoquinone radical couple, which in turn will have direct effect on superoxide radical generation and cytotoxic activity, however as there are only first three members in the homologated series show cytotoxic activity, formation of naphthoquinone radicals may not be the prime mechanism which will lead to cytotoxic activity of these compounds to the cell lines under investigation. Thus, there will be more than one mechanism involved in cytotoxic activity of these compounds. Increase in alkyl groups in side chain length in L-4 to L-8 may restrict their interactions with DNA or other biomolecules of the cell line under investigation. Besides redox cycling of naphthoquinones, their optimum size and noncovalent interactions with DNA are also important factors, which will determine their biological activity [20,21].

## Acknowledgement

SSG grateful BRNS, India and VBK, SSG to RGYI grant of DBT, India for financial support.

## Appendix A. Supplementary material

Figs. S1–S6, crystallographic Tables S1–S3. Crystallographic data have been deposited with the Cambridge Crystallographic Data Centre and may be obtained on request quoting the deposition number CCDC 925343 & 925344 for L-4 and L-8 respectively and 924571 for L-6, from the CCDC, 12 Union Road, Cambridge CB21EZ, UK (Fax: +44 1223 336 033; Email address: deposit@ccdc.cam.ac.uk). Supplementary data associated with this article can be found, in the online version, at <http://dx.doi.org/10.1016/j.molstruc.2013.06.062>.

## References

- (a) E.N. da Silva Junior, C.F. de Deus, B.C. Cavalcanti, C. Pessoa, L.V. Costa-Lotufo, R.C. Montenegro, M.O. de Moraes, M.F.R. Pinto, C.A. de Simone, V.F. Ferreira, M.O.F. Goulart, C.K.Z. Andrade, A. Pinto, *J. Med. Chem.* 53 (2010) 504–508; (b) V.K. Tandon, H.K. Maurya, N.N. Mishra, P.K. Shukla, *Eur. J. Med. Chem.* 44 (2009) 3130–3137; (c) S. Ganapaty, P.S. Thomas, G. Karagianis, P.G. Waterman, R. Brun, *Phytochemistry* 67 (2006) 1950–1956; (d) T.M.S. Silva, C.S. Camara, T.P. Barbosa, A.Z. Soares, L.C. da Cunha, A.C. Pinto, M.D. Vargas, *Bioorg. Med. Chem.* 13 (2005) 193–196; (e) C. Biot, H. Bauer, R.H. Schirmer, E. Davioud-Charret, *J. Med. Chem.* 47 (2004) 5972–5983.
- (a) D.R. da Rocha, A.C.G. de Souza, J.A.L.C. Resende, W.C. Santos, E.A. dos Santos, C. Pessoa, M.O. de Moraes, L.V. Costa-Lotufo, R.C. Montenegro, V.F. Ferreira, *Org. Biomol. Chem.* 9 (2011) 4315–4322; (b) V.R. Campos, E.A. dos Santos, V.F. Ferreira, R.C. Montenegro, M.C.B.V. De Souza, L.V. Costa-Lotufo, M.O. de Moraes, A.K.P. Regufe, A.K. Jordao, A.C. Pinto, J.A.L.C. Resende, A.C. Cunha, *RSC Advances* 2 (2012) 11438–11448; (c) S.J. Lucas, R.M. Lord, R.L. Wilson, R.M. Phillips, V. Sridharan, P.C. McGowan, *Dalton Trans.* 41 (2012) 13800–13802; (d) E. Perez-Sacau, R.G. Diaz-Penata, A. Estevez-Braun, A.G. Ravelo, J.M. Garcia-Castellano, L. Pardo, M. Campillo, *J. Med. Chem.* 50 (2007) 696–706; (e) K.K.C. Liu, J. Li, S. Sakya, *Mini-Rev. Med. Chem.* 4 (2004) 1105–1125; (f) Y. Kumagai, Y. Shinkai, T. Miura, A.K. Cho, *Annu. Rev. Pharmacol.* 52 (2012) 221–247; (g) M. Hallak, B.K. Thakur, Winn, O. Shpilberg, S. Bittner, Y. Granot, I. Levy, L. Nathan, *Anticancer Research* 33 (2013) 183–190; (h) A. Ventura Pinto, S. Lisboa de Castro, *Molecules* 14 (2009) 4570–4590.
- V.K. Tandon, R.B. Chhor, R.V. Singh, S. Rai, D.B. Yadav, *Bioorg. Med. Chem. Lett.* 14 (2004) 1079–1083.
- C.K. Ryu, J.Y. Shim, M.J. Chae, I.H. Choi, J. Han, O. Jung, J.Y. Lee, S.H. Jeong, *Eur. J. Med. Chem.* 40 (2005) 438–444.
- V.K. Tandon, H.K. Maurya, N.N. Mishra, P.K. Shukla, *Eur. J. Med. Chem.* 44 (2009) 3130–3137.
- (a) M.W. Singh, A. Karmarkar, N. Barooah, J.B. Baruah, Belestijn *J. Org. Chem.* 3 (2007) 10; (b) S. Salunke-Gawali, L. Kathawate, Y. Shinde, V.G. Puranik, *J. Mol. Struct.* 1010 (2012) 38–45; (c) S. Rane, K. Ahmed, S. Salunke-Gawali, S.B. Zaware, D. Srinivas, R. Gonnade, M. Bhadbhade, *J. Mol. Struct.* 892 (2008) 74–83; (d) S. Salunke-Gawali, S.Y. Rane, V.G. Puranik, C. Guyard-Duhayan, F. Varret, *Polyhedron* 23 (2004) 2541–2547.
- D.D. Perrin, W.L. Armarego, D.R. Perrin, *Purification of Laboratory Chemicals*, Pergamon Press, London, 1988, pp. 260.
- G.M. Sheldrick, SADABS, Bruker–Siemens Area Detector Absorption and Other Correction, University of Göttingen, Germany, 2006, Version 2008/1.
- ShelXTL 6.14 Bruker AXS Inc., Madison, WI, USA 2003.
- G.M. Sheldrick, SHELX-97 Program for crystal structure solution and refinement, University of Göttingen, Germany, 1997.
- V.B. Konkimalla, T. Efferth, *Biochem. Pharmacol.* 15 (2010) 1092–1099.
- A.T. Dharmaraja, T.K. Dash, V.B. Konkimalla, H. Chakrapani, *Med. Chem. Commun.* 3 (2012) 219–224.
- V.F. Ferreira, S.B. Ferreira, F. de Carvalho da Silva, *Org. Biomol. Chem.* 8 (2010) 4793–4802.
- (a) T.J. Monks, D.C. Jones, *Curr. Drug Metab.* 3 (2002) 425–438; (b) E.V.M. Santos, J.W.M. Carneiro, V.F. Ferreira, *Bioorg. Med. Chem.* 12 (2004) 87–93; (c) A. Brunmark, E. Cadenas, *Free Radical. Biol. Med.* 7 (1989) 435–477; (d) T.J. Monks, R.P. Hanslik, G.M. Cohen, D. Ross, D.G. Graham, *Toxicol. Appl. Pharmacol.* 112 (1992) 2–16; (e) J.L. Bolton, M.A. Trush, T.M. Penning, G. Dryhurst, T.J. Monks, *Chem. Res. Toxicol.* 13 (2000) 135–160; (f) A.B. Pardee, Y.Z. Li, C.J. Li, *Curr. Cancer Drug Targets* 2 (2002) 227–242; (g) S.B. Ferreira, D.T.G. Gonzaga, W.C. Santos, K.G.L. Araujo, V.F. Ferreira, *Rev. Virtual Quim.* 2 (2010) 140–160; (h) M.N. da Silva, V.F. Ferreira, M.C.B.V. de Souza, *Quim. Nova* 26 (2003) 407–416.
- (a) V.H.J. Frade, M.J. Sousa, J.C.V.P. Moura, M.S.T. Gonçalves, *Bioorg. Med. Chem.* 16 (2008) 3274–3282; (b) K.I.E. McLuckie, Z.A.E. Waller, D.A. Sanders, D. Alves, R. Rodriguez, J. Dash, G.J. McKenzie, A.R. Venkitaraman, S. Bolsubramanian, *J. Am. Chem. Soc.* 133 (2011) 2658–2663.
- K.-Y. Chu, J. Griffiths, *J. Chem. Soc. Perkin Trans. 1* (1978) 1083–1087.
- (a) C.G. Pierpont, *Coord. Chem. Rev.* 216–217 (2001) 99–125; (b) C.G. Pierpont, C.W. Lange, *Inorg. Chem.* 41 (1994) 381–492.
- (a) J. Gaultier, C. Hauw, *Acta Crystallogr.* 19 (1965) 585–590; (b) A.E. Shvets, A.J. Malmanis, Ya.F. Freimanis, Ya.F. Bleidelis, J.F. Dregeris, *Zh. Strukt. Khim.* 20 (1979) 414–419; (c) V. Bertolasi, P. Gilli, V. Ferretti, G. Gilli, *Acta Crystallogr. Sec. B: Struct. Sci.* 51 (1995) 1004–1015; (d) A.E. Shvets, Ya.F. Bleidelis, Ya.F. Freimanis, *Zh. Strukt. Khim.* 16 (1975) 640–644; (e) D.E. Lynch, I. McClenaghan, *Acta Crystallogr. E* 57 (2001) o287–o288 (Acta

Crystallogr. C: Cryst. Struct. Commun. 56 (2000) e537. Acta Crystallogr., Sec. C: Cryst. Struct. Commun. 56 (2000) e588. Acta Crystallogr., Sec. E: Struct. Rep. Online 59 (2003) o1427);  
(f) F.-L. Yang, T. Win, S. Bittner, Z. Kristallogr, New Cryst. Struct. 220 (2005) 173;  
(g) Y. Brandy, R.J. Butcher, T.A. Adesiyun, S. Berhe, O. Bakare, Acta Crystallogr. Sec. E: Struct. Rep. Online 65 (2009) o64.

[19] G.R. Desiraju, J.J. Vittal, A. Ramanan, Crystal Engineering, World Scientific Publishing Co. Pvt. Ltd., 2011.  
[20] A. Bolognese, G. Correale, M. Manfra, A. Lavecchia, E. Novellino, S. Pepe, J. Med. Chem. 49 (2006) 5110–5118.  
[21] A. Bolognese, G. Correale, M. Manfra, A. Lavecchia, O. Mazzoni, E. Novellino, V. Barone, A. Pani, E. Tramontano, P. La Colla, C. Murgioni, I. Serra, G. Setzu, R. Loddo, J. Med. Chem. 45 (2001) 5205–5216.